# Photogrammetrically Measured Distortions of Composite Microwave Reflector System in Vacuum at ~90K

Peter Mulé, Michael D. Hill, Henry P. Sampler

Goddard Space Flight Center, Greenbelt Maryland

**ABSTRACT**

The Microwave Anisotropy Probe (MAP) Observatory, scheduled for a late 2000 launch, is designed to measure temperature fluctuations (anisotropy) and produce a high sensitivity and high spatial resolution (better than 0.3° at 90 GHz.) map of the Cosmic Microwave Background (CMB) radiation over the entire sky between 22 and 90 GHz. MAP utilizes back-to-back composite Gregorian telescopes supported on a composite truss structure to focus the microwave signals into 10 differential microwave receivers. Proper position and shape of the telescope reflectors at the operating temperature of ~90 K is a critical element to ensure mission success.

We describe the methods and analysis used to validate the in-flight position and shape predictions for the reflectors based on photogrammetric metrology data taken under vacuum with the reflectors at ~90K. Contour maps showing reflector distortion were generated. The resulting reflector distortion data are shown to be crucial to the analytical assessment of the MAP instrument's microwave system in-flight performance.

**KEY WORDS:** reflectors, distortions, and photogrammetry

## 1. Introduction

The MAP instrument is designed to measure the anisotropy of the Cosmic Microwave Background (CMB) radiation over the full sky while operating at a temperature of approximately 90K. The instrument's Thermal Reflector System (TRS) consist of back-to-back Gregorian telescopes with reflectors manufactured by Programmed Composite Incorporated (PCI) of Anaheim California, and are constructed of SF-70A-75/RS-12D facesheets with a shaped Korex core sandwich bonded with a FM-73 film adhesive. Each reflector has an aluminum honeycomb backing structure with XN-70A/RS-3 facesheets. The truss structure on which the reflectors are mounted is constructed of XN-70A/RS-3 and M46J/RS-3 flat laminates bonded with EA 9394 adhesive.

Figure 1 shows the positions of the primary and secondary reflectors on the composite truss structure comprising the Thermal Reflector System (TRS). A flight unit as well as a Reflector Engineering Unit (REU) was manufactured identical except that the REU included only one reflector pair and part of the truss on the opposing side was removed. Both the flight TRS and the REU were instrumental in characterizing the reflector system.

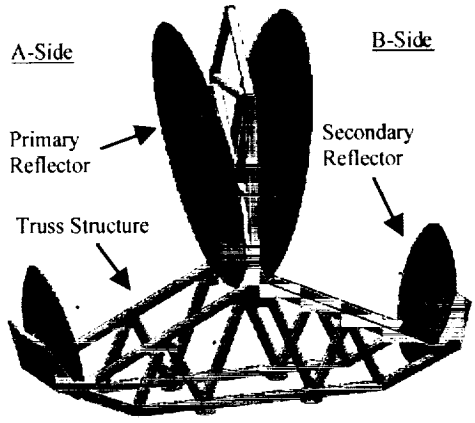


Figure 1: Thermal Reflective System (TRS)

# Photogrammetrically Measured Distortions of Composite Microwave Reflector System in Vacuum at ~90K

Peter Mulé, Michael D. Hill, Henry P. Sampler

Goddard Space Flight Center, Greenbelt Maryland

**ABSTRACT**

The Microwave Anisotropy Probe (MAP) Observatory, scheduled for a late 2000 launch, is designed to measure temperature fluctuations (anisotropy) and produce a high sensitivity and high spatial resolution (better than 0.3° at 90 GHz.) map of the Cosmic Microwave Background (CMB) radiation over the entire sky between 22 and 90 GHz. MAP utilizes back-to-back composite Gregorian telescopes supported on a composite truss structure to focus the microwave signals into 10 differential microwave receivers. Proper position and shape of the telescope reflectors at the operating temperature of ~90 K is a critical element to ensure mission success.

We describe the methods and analysis used to validate the in-flight position and shape predictions for the reflectors based on photogrammetric metrology data taken under vacuum with the reflectors at ~90K. Contour maps showing reflector distortion were generated. The resulting reflector distortion data are shown to be crucial to the analytical assessment of the MAP instrument's microwave system in-flight performance.

**KEY WORDS:** reflectors, distortions, and photogrammetry

## 1. Introduction

The MAP instrument is designed to measure the anisotropy of the Cosmic Microwave Background (CMB) radiation over the full sky while operating at a temperature of approximately 90K. The instrument's Thermal Reflector System (TRS) consist of back-to-back Gregorian telescopes with reflectors manufactured by Programmed Composite Incorporated (PCI) of Anaheim California, and are constructed of SF-70A-75/RS-12D facesheets with a shaped Korex core sandwich bonded with a FM-73 film adhesive. Each reflector has an aluminum honeycomb backing structure with XN-70A/RS-3 facesheets. The truss structure on which the reflectors are mounted is constructed of XN-70A/RS-3 and M46J/RS-3 flat laminates bonded with EA 9394 adhesive.

Figure 1 shows the positions of the primary and secondary reflectors on the composite truss structure comprising the Thermal Reflector System (TRS). A flight unit as well as a Reflector Engineering Unit (REU) was manufactured identical except that the REU included only one reflector pair and part of the truss on the opposing side was removed. Both the flight TRS and the REU were instrumental in characterizing the reflector system.

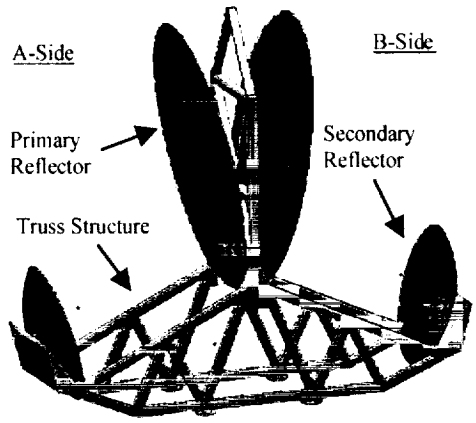


Figure 1: Thermal Reflective System (TRS)

Accurate predictions of in-flight reflector distortion and position values were necessary to predict instrument performance. Distortion and position values are input into the YRS Inc. Diffraction Analysis for Dual Reflector Analysis (DADRA) code that provides predictions of flight performance. Distortion were initially derived with finite element analysis by applying flight temperatures to the structural finite element model. In parallel, we were investigating photogrammetry as a technique to verify the reflector shapes during thermal vacuum testing. A close range photogrammetry system[1] used to acquire precise coordinates from photographs was acquired and initially used during the Reflector Engineering Unit (REU) thermal vacuum testing. Dramatic differences in Finite Element Model (FEM) and photogrammetrically (PG) measured shapes were realized (Figure 2). Attempts to correlate the FEM were unsuccessful. Photogrammetry was adopted as the method of deriving TRS reflector shape and point position values for flight performance analysis.

Figure 2: REU Primary Reflector FEM vs Photogrammetry Deformations from Ideal at ≈90K
(Plots are of z-axis deformation in the reflector coordinate system)

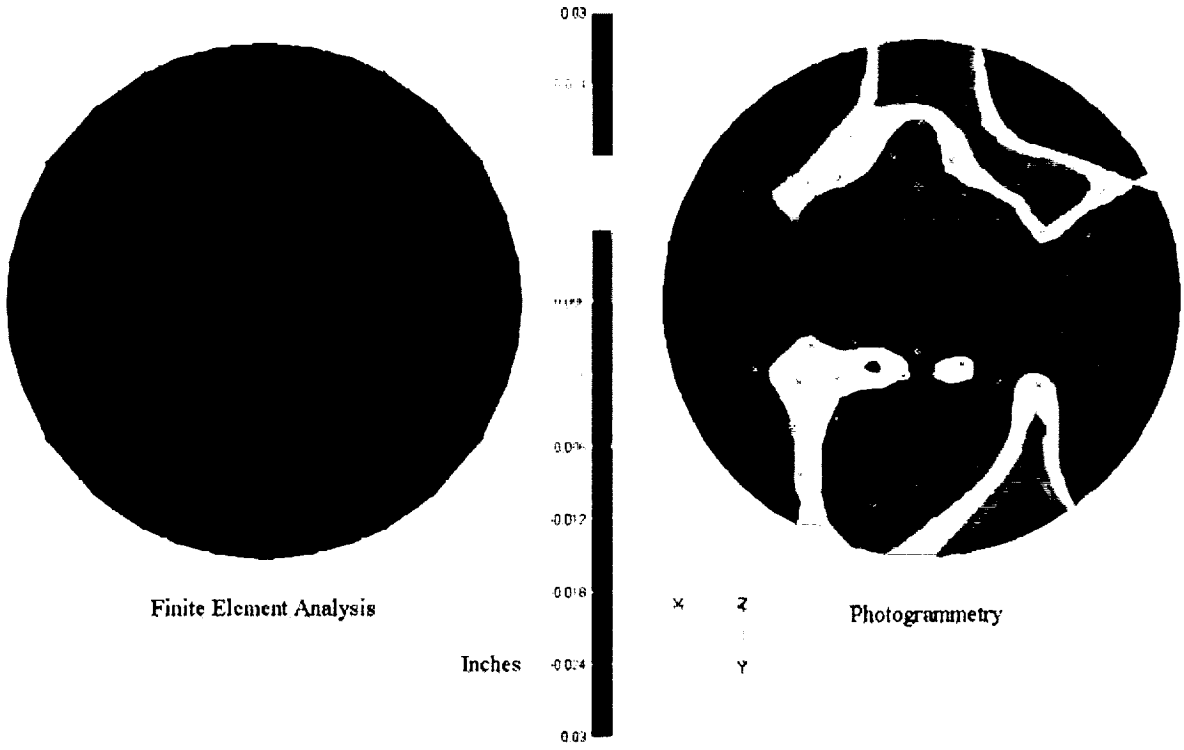


The desired surface figures (ideal) and selected point positions were defined and verified at room temperature by the manufacturer of the REU and TRS. The manufacturer performed a continuous surface scan with an SMX laser tracker prior to coating the surfaces and subsequent integration of the reflectors as a telescope unit. Tooling ball reference targets were added to each reflector and valued with coordinates relative to the reflectors surface figure and the ideal relative positions of the reflectors to each other. The reflector tooling ball coordinates when cold (with warm offset) were used to align the reflectors in a local instrument reference frame during integration at room temperature. Tooling hole boss (THB) targets on the TRS truss structure were also added and valued in the local instrument reference frame to provide a means of reestablishing the coordinate reference frame after removing the tooling ball targets on the reflectors. A combination of the warm atmospheric pressure and cold vacuum PG measurements, the defined ideal surface figure, and a knowledge of the warm surface positions with respect to ideal (from the TRS manufacturer), allowed us to describe the reflector positions under flight-like conditions. The DADRA code was then used to analyze the effects of the relative positions and distortions of the reflectors on the optical performance.

## 2. Photogrammetry Measurements

The measurements reported here were acquired from retro-reflective photogrammetry targets designed to be placed in the THBs and for stick-on photogrammetry retro-reflective targets placed on the front surfaces of the reflectors (two primaries -35 targets each, 2 secondaries-13 targets each). Measurements were performed at atmospheric pressure and ambient temperature and in vacuum at ambient and cold temperatures (Table 1). The photogrammetry camera used to make the measurements was mounted in a thermally controlled canister on a carousel mounted atop a helium shroud surrounding the TRS. The carousel was remotely operated to position the camera in 42 locations and 2 orientations to allow for triangulation and resection of target coordinates and camera positions in the photographs taken. Target positions were measured with a precision of 0.002 inches.

Table 1: TRS Photogrammetry Test Conditions

| PG Run | Pressure | Temp (K) | Comments |
|---|---|---|---|
| 1 | Atmospheric | 290 | Established reflector target baseline values |
| 2 | Vacuum | 290 | Identified effects of vacuum (none) |
| 3 | Vacuum | 91 | First cold deformation case |
| 4 | Vacuum | 95 | Second cold deformation case |
| 5 | Atmospheric (N2) | 294 | Identify residual effects of thermal vacuum cycling (none) |

To verify the precision of the PG system measurements, ambient temperature and pressure PG measurements of the TRS THB targets were compared with measurements made with a Leica Laser Tracker (LT) system and measurements made with a theodolite network system (the Analytic Industrial Metrology System (AIMS)). The three-metrology systems agreed to within 0.007 inches (0.178 mm). The PG system measurements when compared to each other were repeatable to 0.002 inches (0.051 mm) and agreed with the values established in the final Laser Tracker measurements performed at the telescope's manufacturer.

Analysis of the deformations of the TRS in thermal vacuum required only minor changes in the methods of establishing the local instrument coordinate reference frame. The low coefficient of thermal expansion (CTE) and symmetry of the truss structure allowed the use of room temperature THB coordinates on the truss when performing a transformation of coordinates into the local coordinate reference frame. The truss THB targets were located symmetrically such that no biasing would occur in their alignment when cold. Vertical translations of the truss at its Titanium flexure interface due to flexure contraction (0.0046 inches (0.117 mm)) were noted. The final coordinates when cold were established by least squares fitting the truss THB targets to the room temperature baseline values, scaling back using scale-bars of known CTE and temperature (the scale factor was very near 1 confirming a low CTE for the truss), and applying predicted flexure contraction translation.

## 3. Reflector Distortions

Figure 3 shows the placement scheme of the PG targets on the surfaces of the TRS primary and secondary reflectors. Contamination concerns restricted the number and location of surface targets. Target locations were chosen to best describe the overall distortion based on the distortion pattern identified during Reflector Engineering Unit (REU) testing. Targets were not placed on the upper portion of the secondary reflector because the camera could not view it in the test configuration.

Figure 3: PG Target Positions on Primary Reflector 2R and Secondary Reflector 2

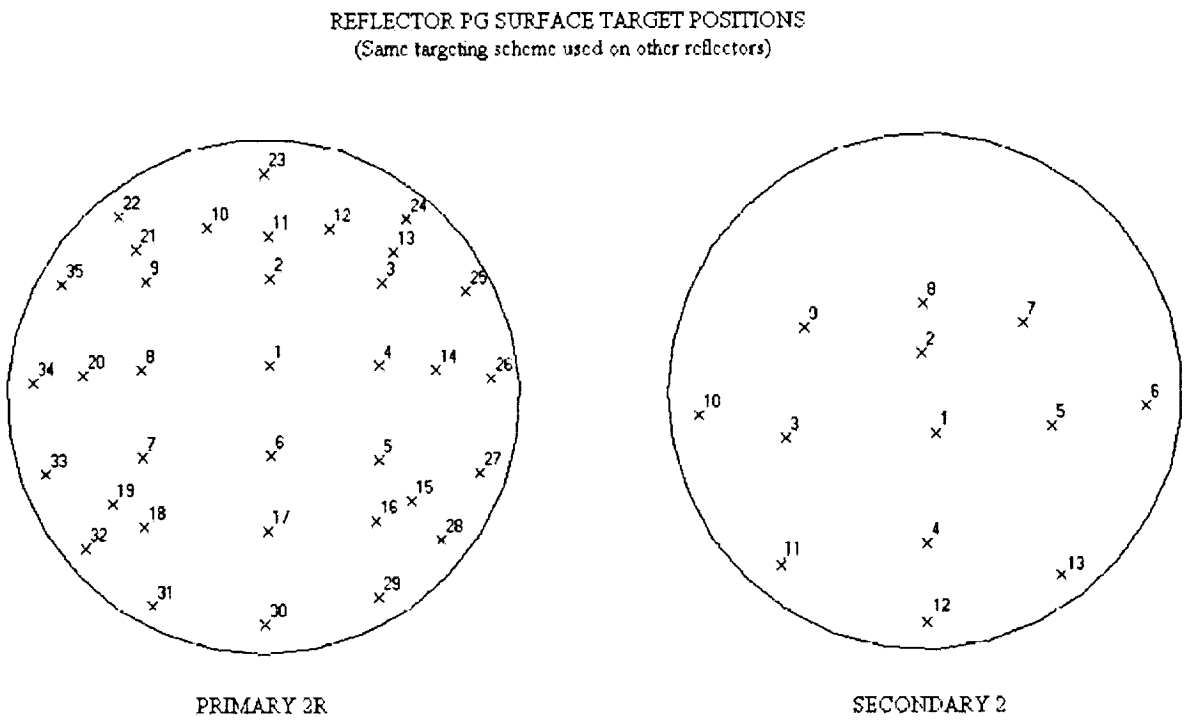


To develop a description of the distortions of the primary reflectors when cold the following process was used:

1. The measured coordinates of the reflector targets when cold were least squares fit to their warm positions. This placed the cold surface in a position known with respect to the ideal surface positions.
2. Knowledge of the reflector warm surface position with respect to ideal, (from telescope manufacturer data) allowed us to transform positions from step 1 to ideal. Steps 1 and 2 provided knowledge of the measured reflector cold positions with respect to ideal.
3. The target positions were then compared with the ideal surface using Imageware surface fitting software. A shift in the standing axis direction was allowed to partially correct for the 0.010-inch (0.254 mm.) target thickness.
4. Residuals from the least squares fit) from step 3 were used to develop distortion values in the reflector local coordinate reference frame (format required for DADRA code).
5. Fine grid interpolation was done using NASTRAN modeling. DADRA requires a x, y, and dz input so that an interpolation of dz could be done using a flat plate model with enforced displacement.

As a check of the photogrammetric measurements, the warm distortions measured with the PCI laser tracker were compared with the distortions measured with the photogrammetric camera. Table 2 is a summary of LT and PG based surface distortions for the TRS primary reflectors. This comparison highlights differences in the outer annulus that has the largest unsupported areas and the least stiff backing structure. The differences are likely due to relaxation of the reflector material between the initial LT measurement and the PG measurement. LT measurements were made prior to the surface coating and integration.

Table 2: TRS Primary Reflector RMS Distortion Summaries (i)

| | Primary 2R | | | Primary 3 | | |
|---|---|---|---|---|---|---|
| | r < 9.8 | 9.8< r <19.7 | r > 19.7 | r < 9.8 | 9.8< r <19.7 | r > 19.7 |
| Requirement | 0.0015 | 0.0020 | 0.0030 | 0.0015 | 0.0020 | 0.0030 |
| LT Warm + (ii) | 0.0024 | 0.0021 | 0.0034 | 0.0018 | 0.0017 | 0.0031 |
| PG Warm (iii) | 0.0024 | 0.0024 | 0.0052 | 0.0022 | 0.0037 | 0.0060 |
| PG Cold (iii) | 0.0069 | 0.0053 | 0.0117 | 0.0047 | 0.0064 | 0.0111 |

(i) Values represent surface normal errors. Distortion contour plots represent z component error of the optical coordinate system.
(ii) LT measured points and additional derived points included for more uniform and complete distribution.
(iii) PG measured points and additional derived points included.

Table 3 below is a summary of secondary surface target residuals in the local coordinate reference frame of the TRS after least squares fitting to the warm data. The small residuals agree with measurements made on the REU.

Table 3: TRS Secondary Cold Fit to Warm PG Residuals (*)

| | Secondary SN 2 | | | Secondary SN 3 | | |
|---|---|---|---|---|---|---|
| No. of Targets | 9 | | | 8 | | |
| | dX | dY | dZ | dX | dY | dZ |
| Standard Deviation | 0.0012 | 0.0015 | 0.0009 | 0.0021 | 0.0008 | 0.0010 |
| Minimum | -0.0025 | -0.0027 | -0.0010 | -0.0040 | -0.0010 | -0.0018 |
| Maximum | 0.0015 | 0.0022 | 0.0015 | 0.0030 | 0.0013 | 0.0011 |

(*) Three upper targets on the secondary reflectors were at extreme angles and in limited number of photos. These targets were not included in summary.

Contour maps were created to visually represent the distortions of the reflectors. The contours represent actual to ideal surface deviations in the z axes of the reflector coordinate system. The local coordinate axes for the reflectors can be seen in Figure 4. DADRA code requires the x, y, delta z format. Figure 5 shows the relations between the surface normal and the reflector z translation direction for a single point. An Ideal reflector would appear as a flat disc of uniform color. Images are orientated such that we are looking at the reflective surface along an axis nearly parallel with the individual reflector z-axis (a slight x-axis rotation is applied to provide view of distortion). The offset angles is used in the images to give a better idea of the distortion patterns and does not show reflector shape.

Figure 4: Reflector Coordinate Systems

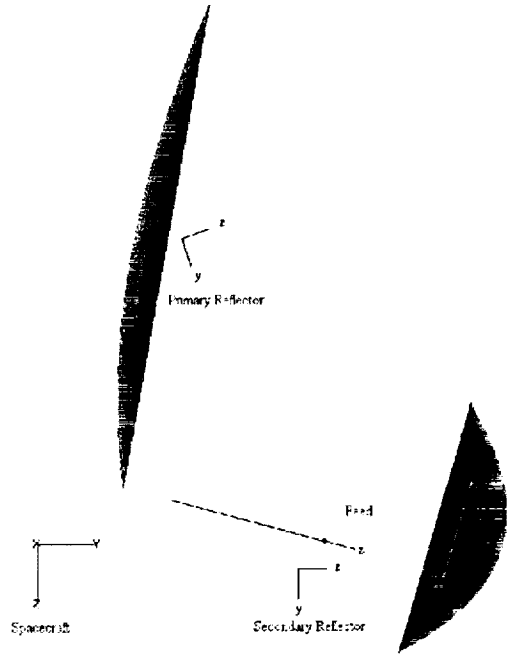


Figure 5: Relations between Surface Normal and Reflector dZ for a single point in the local area of the point

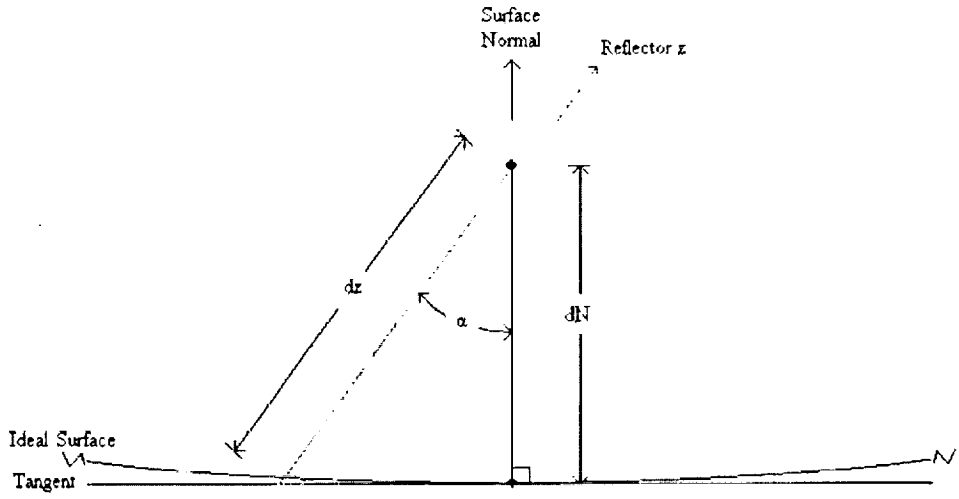


dn - Normal distance to ideal surface
dz - Distance from measured target to ideal surface along reflector z axis
α Angle between surface normal and reflector z axis
● - Measured target position on actual reflector
● - Ideal surface point with surface normal passing through measured target

The contour maps in figure 6 show warm (as-built) distortions of primary reflector 2R as derived from laser tracker and photogrammetry measurements. The 35 PG targets produce a relatively good representation of the distortion over the entire surface. LT data consisted of approximately 1000 points distributed over the entire surface. Differences in these images, and those for reflector SN 3, are mainly near the outer perimeter and are likely due to extrapolation in areas of high distortion gradient and minor changes in the reflectors shape during the processing following the initial LT measurements.

Figure 6: Primary Reflector 2R Laser Tracker and PG Camera Comparisons (Warm)

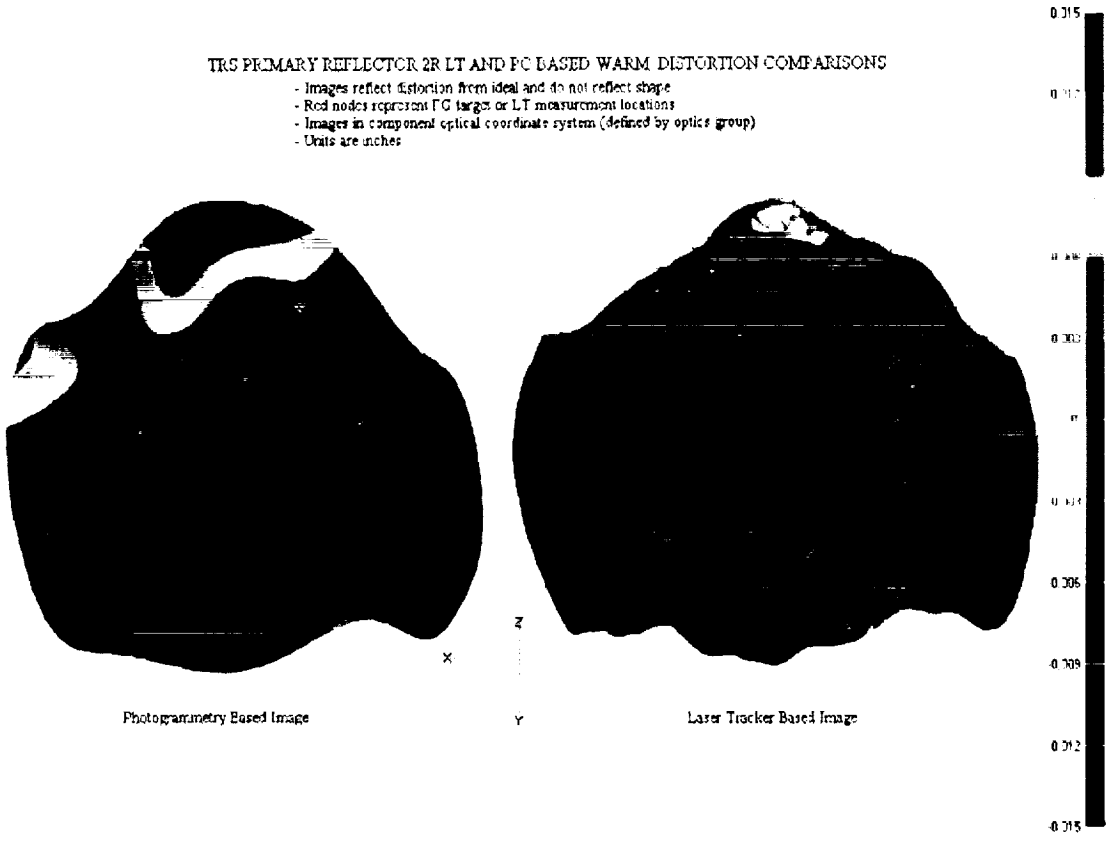

The contour maps in figure 7 show warm (as-built) distortions of primary reflector 3 as derived from laser tracker and photogrammetry measurements. There is an apparent difference in the lower section of the contour maps. Later THB measurements show the balls in this area to be out of position by approximately 0.010 inches when compared to the baseline data measured prior to delivery of the reflector system. The TB offsets therefor support the PG surface measurements and distortion trends.

Figure 7: Primary Reflector 3 Laser Tracker and PG Camera Measurements (Warm)

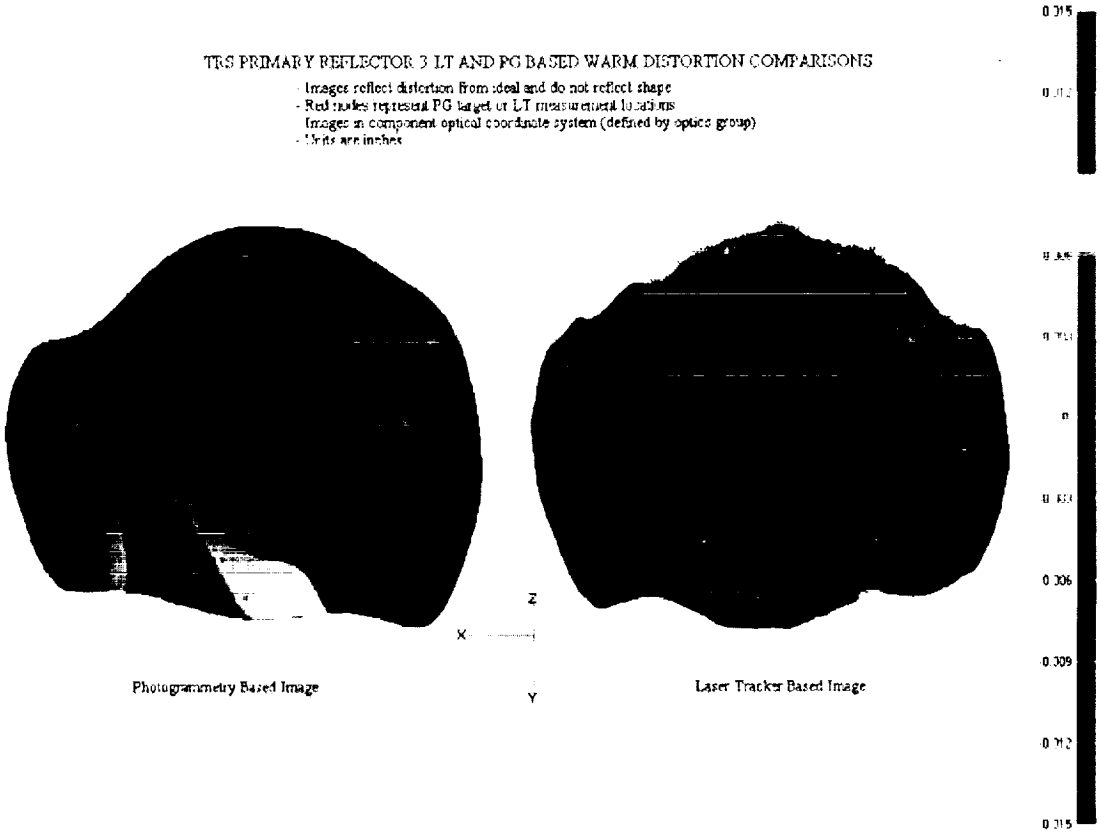

The contour maps in Figure 8 shows the primary reflector distortions based on the cold PG data. The distortions when cold are nearly identical for the two reflectors. These images reflect the DADRA distortion input values used to predict flight performance.

Figure 8: TRS Primary Reflectors PG Measured Distortions at 90K

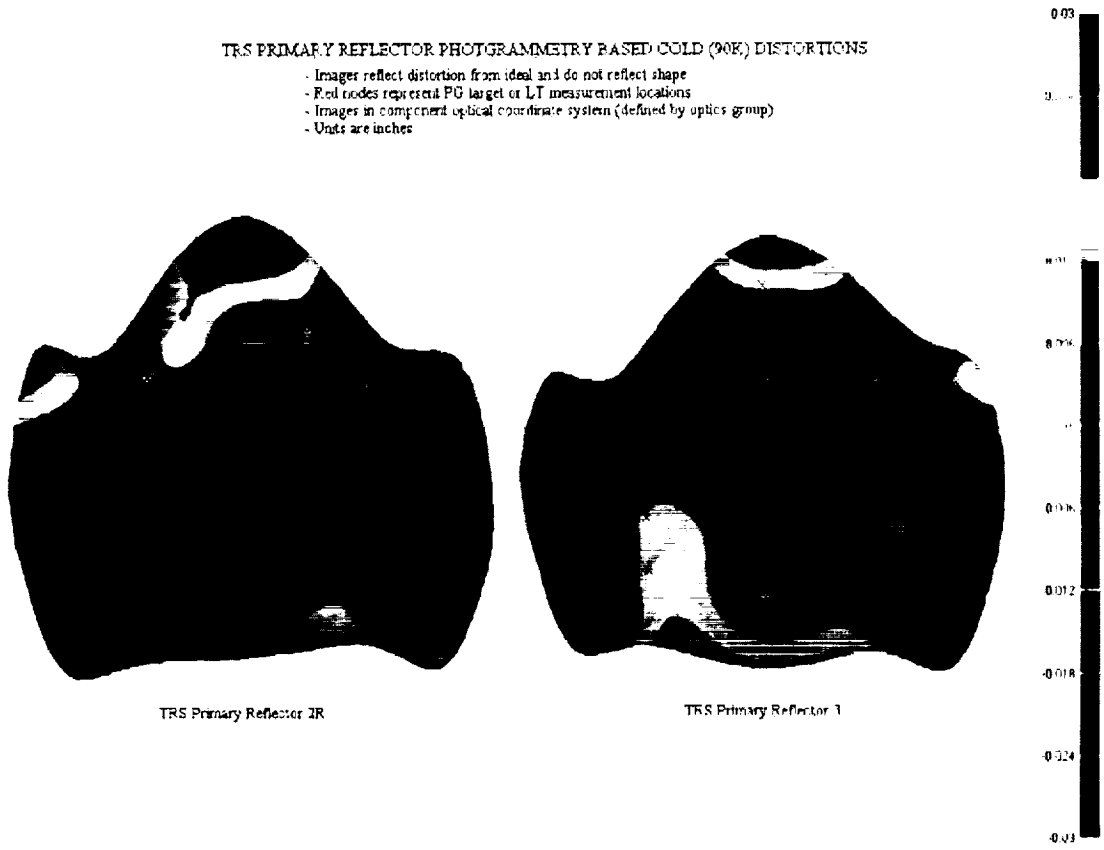

The contour maps in figure 9 were created from the PG measurements performed on the REU in a cold vacuum environment. These are included to show the similarity to TRS distortions and how a reduced number of targets were able to create a good shape. When compared to the TRS cold images it revealed that a hat ring stiffener added to the outer perimeter of the TRS reflectors slightly reduced the distortion along the outer rim, especially in the middle and upper rim areas where the ring properties were the stiffest. The primary reflector backing rib pattern is apparent in this cold distortion image.

Figure 9: PG Camera Measurements at Room Temperature and at 90K

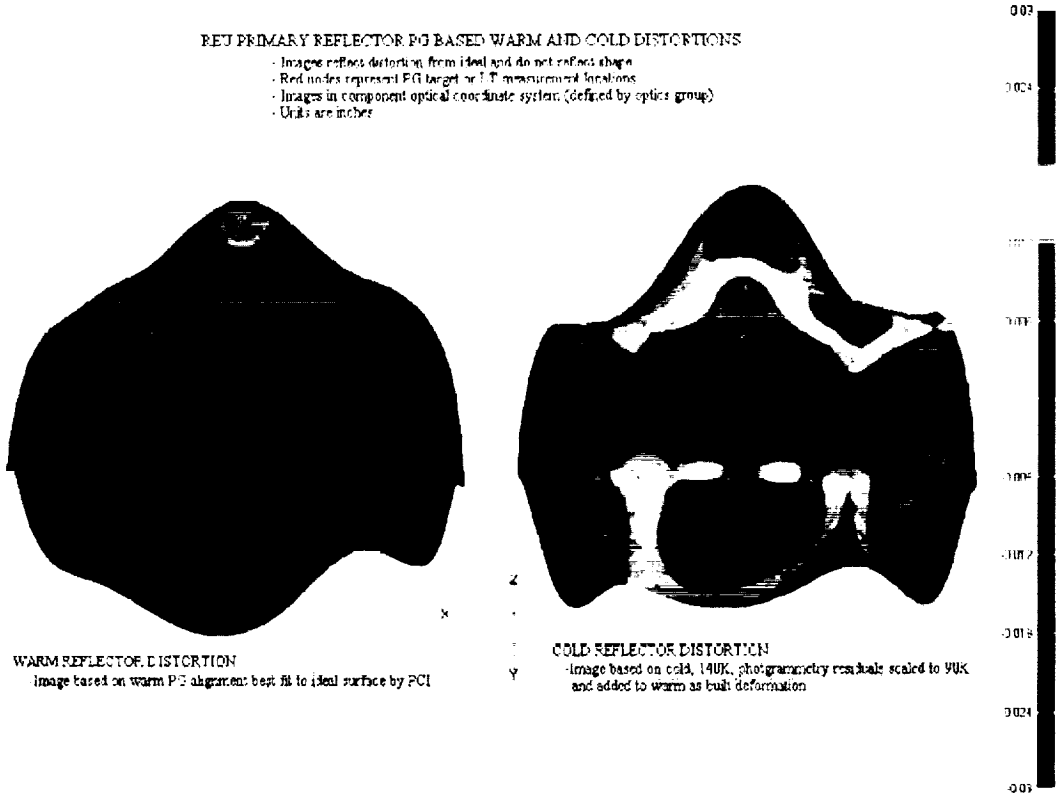

The secondary reflector contour maps of figure 10 are based on the REU measurements. The secondary reflector surface was completely targeted (81 PG target positions marked) for the REU testing. The images show that the overall distortion of the secondary after the cold transition is negligible supporting the limited TRS secondary reflector measurements.

Figure 10: REU Secondary Reflector PG Measurement Distortion Contour Maps

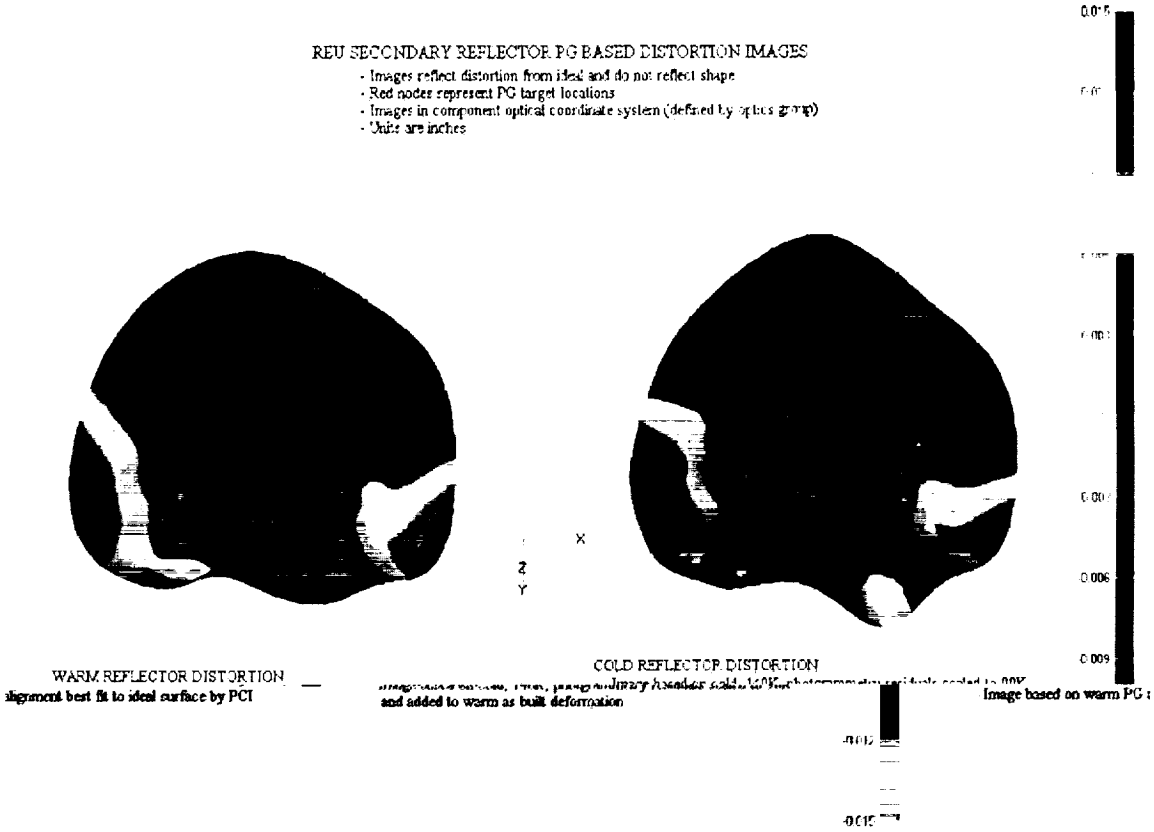

## 4. Photogrammetry Based Performance Predictions

The TRS reflector shape and position data were incorporated into the DADRA input to develop the flight performance predictions for the MAP instrument. Secondary reflector warm distortions were used for flight predicts since negligible distortion was measured and full surface shapes could not be obtained. Flight performance predictions were within the criteria set by MAP systems engineering analysis. A comparison of ground test results and DADRA predictions was made to give confidence to the combination of the PG measured shape and position predictions and the DADRA code. The comparison showed excellent agreement between measurements and predictions (Table 4).

Table 4: Comparison of Test and Analytical Performance at Ambient

| Position | Pointing [1] | | | | Beam Size | | | |
|---|---|---|---|---|---|---|---|---|
| | Elevation (°) | | Azimuth (°) | | X-Beam FWHM (°) | | Y-Beam FWHM (°) | |
| | Test | Analysis | Test | Analysis | Test | Analysis | Test | Analysis |
| KalA | -22.26 | -22.28 | -2.34 | -2.34 | 0.551 | 0.561 | 0.684 | 0.672 |
| Q2A | -17.77 | -17.77 | 1.97 | 1.97 | 0.569 | 0.543 | 0.491 | 0.469 |
| V2A | -19.66 | -19.69 | 2.04 | 2.03 | 0.304 | 0.317 | 0.307 | 0.313 |
| W2A | -19.04 | -19.04 | -0.56 | -0.56 | 0.190 | 0.205 | 0.187 | 0.191 |
| W4A | -20.14 | -20.16 | 0.60 | 0.61 | 0.202 | 0.210 | 0.201 | 0.208 |
| KalA | -22.26 | -22.27 | -2.42 | -2.43 | 0.549 | 0.560 | 0.690 | 0.672 |
| Q2A | -17.72 | -17.72 | 1.95 | 1.92 | 0.573 | 0.541 | 0.491 | 0.465 |
| V2A | -19.65 | -19.64 | 2.00 | 2.03 | 0.293 | 0.313 | 0.304 | 0.306 |
| W2A | -19.05 | -19.01 | -0.61 | -0.62 | 0.189 | 0.201 | 0.189 | 0.193 |
| W4A | -20.13 | -20.11 | 0.55 | 0.55 | 0.193 | 0.205 | 0.199 | 0.207 |

(1) Test pointing values correct for approximated offset in chamber boresight

## 5. Conclusions

Photogrammetric measurements have allowed us to obtain the shape and position values of our reflectors in vacuum at cryogenic temperatures. Empirical cold shape data were a significant improvement over analytical predictions and also highlighted shape errors due to fabrication where analytical predictions assume a perfect initial shape. When compared to Laser Tracker metrology, photogrammetric measurements captured the as built distortions of the reflectors and identified a possible relaxation of the reflector material. Photogrammetry together with beam mapping and DADRA code enabled us to quantify and qualify the ground and on-orbit characteristics of the microwave reflectors.
Significant time went into developing a method to safely target the coated flight reflectors and we do not advise sticking targets directly on your reflective surfaces.


### Acknowledgments

The authors would like to thank Acey Hererra (Swales and Associates), John Brown (Geodetic Services, Inc.), Programmed Composite, Inc., and John Beggs (GSFC)


### References


1. Automation in Digital Close-Range Photogrammetry, Clive S. Fraser, First Trans Tasman Surveyors Conference, 12-18 April, 1997, New Castle